PERGAMON

International Journal of Solids and Structures 38 (2001) 3673–3687

INTERNATIONAL JOURNAL OF SOLIDS and STRUCTURES

www.elsevier.com/locate/ijsolstr

Higher-order theories for thermal stresses in layered plates

Klaus Rohwer [a,*], Raimund Rolfes [a], Holger Sparr [b]

[a] *Deutsches Zentrum fur Luft- und Raumfahrt (DLR), Institute of Structural Mechanics, Postfach 3267, D-38022 Braunschweig, Germany*

[b] *TU Dresden, Institute of Solid Mechanics, D-01062 Dresden, Germany*

Received 25 February 2000

Abstract

First order shear deformation theory renders quite accurate in-plane stresses even for rather thick plates. By means of equilibrium conditions derivatives of the in-plane stresses can be integrated to determine transverse shear and normal stresses. The need to use in-plane derivatives requires at least cubic shape functions. Simplifying assumptions relieve these requirements leading to the extended 2D method. While under mechanical load this method yields excellent results, poor transverse normal stresses have been obtained for plates under a sinusoidal temperature distribution. This paper traces back these deficiencies to lentil-like deformations of each separate layer. It is proved that third or fifth order displacement approximations through the plate thickness avoid these deficiencies.

Keywords: Plates; Laminated composites; Transverse stresses; Thermal loads; Lentil-like deformations

1. Introduction

Layered composite plates are often rather slender structures for which in-plane stresses in general can be obtained quite accurately by means of 2D theories. Such theories are based on assumptions concerning the distribution of the displacement functions over the plate thickness. The most simple theories assume linear distributions of the in-plane displacements. Prominent exponents thereof are the classical lamination theory (CLT) and the first-order shear-deformation theory (FSDT) extended to laminates by Whitney and Pagano (1970).

Rohwer (1992) has shown that the FSDT approach is sufficient for determining excellent in-plane stresses even if the plate slenderness is not very high. The use of higher order theories increases the computational effort whereas the gain in accuracy is small. Implementation of higher order theories into finite element approximations often requires $C^{(1)}$-continuity of the shape functions which prevents simple element formulations. If the plate is very thick a full 3D analysis is required anyway. Thus, higher order plate theories are of advantage for in-plane stresses only within a relatively narrow bandwidth of slenderness

* Corresponding author. Tel.: +49-531-295-2384; fax: +49-531-295-2875.
E-mail address: klaus.rohwer@dlr.de (K. Rohwer).

0020-7683/01/$ - see front matter
PII: S0020-7683(00)00249-3

rates. This statement has been proven correct for plates under mechanical loads. It seems logical that a corresponding statement holds also for stresses due to thermal loads if the applied temperature difference and the boundary conditions allow for a linear distribution of in-plane displacements.

In-plane stresses are in many cases fully sufficient to judge upon the structural strength. Layered composite plates, however, show inhomogeneous and anisotropic strength properties. In order to specify their susceptibility to delaminations and other failure modes transverse shear and normal stresses must be known in addition. Different techniques are available to reach that aim. Applying 3D or quasi-3D finite elements is a straight forward but often a rather expensive approach, due to the experience that often three to five elements per layer thickness are necessary to obtain an acceptable accuracy.

To overcome this disadvantage Mau et al. (1972), Spilker et al. (1977) and Spilker (1982) proposed layerwise hybrid-stress elements, where, in general the number of degrees of freedom depends on the number of layers. Based on a layerwise constant shear angle theory Chaudhuri (1986) formulated a triangular plate element. He used equilibrium conditions to determine transverse shear stresses. Owen and Li (1987) started with a piecewise displacement approximation and eliminated internal degrees of freedom by means of a substructuring technique. Robbins and Reddy (1993) developed 2D displacement elements with a layerwise linear, quadratic or cubic displacement approximation through the thickness. In a corresponding approach Gruttmann and Wagner (1994) used layerwise hierarchical polynomials. Differentiation of the resulting displacements and application of the material law lead to the desired transverse stresses; in some cases, smoothing procedures are recommended to reduce discrepancies in the equilibrium conditions at layer interfaces. A detailed assessment of different modeling approaches is recently given by Noor and Malik (2000).

On the other hand, transverse shear and normal stress components can be obtained by means of the 3D equilibrium conditions. To that end, derivatives of the in-plane stress components which can be determined from a simple 2D theory must be integrated over the plate thickness. Noor et al. (1990) applied such a procedure and used the predicted stresses as input for a corrector step where displacements and stresses are adapted to the reduced stiffnesses. Reduced transverse shear stiffnesses can also be determined in advance when introducing simplifying assumptions as proposed by Rohwer (1988). Since this procedure accounts for a more realistic distribution of transverse shear stresses it gives rise to a better approximation than fixed shear correction factors. Local application of equilibrium conditions leads to the extended 2D method which could be shown by Rolfes and Rohwer (1997), Rolfes et al. (1998a) to yield excellent results for transverse shear and normal stresses. Also under thermal loads accurate results can be obtained as Rohwer and Rolfes (1998) demonstrated for instance for an anti-symmetric cross-ply laminate under a temperature gradient. More detailed numerical tests by Rolfes et al. (1998b) revealed, however, that there are cases for which the transverse normal stresses are rather poor, sometimes without any relation to the 3D results. This paper aims at thoroughly investigating these deviations and explaining the reasons. Furthermore, higher order 2D theories are formulated which avoid the deficiencies. Numerical examples demonstrate which degree of approximation in thickness direction is required for determining accurate transverse normal stress distributions from the extended 2D method.

2. Extended 2D method, advantages and deficiencies

2.1. Theoretical basis

Finding a suitable yardstick for a sound and fair judgement upon the accuracy of the extended 2D method is a major problem which must be solved. Test results are not available and would be very difficult to obtain. Therefore, one must cope with 3D elasticity solutions to compare with. Closed form solutions including the transverse stress components are available for simply supported rectangular plates with a

symmetric lay-up by Pagano (1970), Srivinas and Rao (1970) and an antisymmetric lay-up by Noor and Burton (1990). Vel and Batra (1999) have treated rectangular plates with two opposite edges simply supported and eight different boundary conditions satisfied at the other two edges. Solutions are obtained by means of infinite series. However, these solutions are developed for mechanical loads only. Extensions to thermal load are possible but specific boundary conditions must be kept.

On the other hand the third author has had the chance to use a computer program based on the differential quadrature method by Malik and Bert (1998). This numerical method discretizes the considered problem in a so-called quadrature net. Results are extremely close to analytical solutions and are not restricted with respect to boundary conditions. Results obtained with this program will serve as the reference solutions. Coordinate system and plate dimensions are given in Fig. 1. The axes x_1 and x_2 form the reference surface located half way between the upper and lower laminate surface. Fiber angles are specified with respect to the x_1 axis.

Detailed deductions of the extended 2D method can be found in the papers of Rolfes et al. (1998a,b). In the following, the theoretical basis of the method is given in a condensed form. Starting point of the development is the 3D equilibrium condition. Having solved for the transverse stresses results in transverse shear stresses depending on derivatives of in-plane stresses,

$$\sigma_{\alpha 3} = -\int_{\varsigma=-h/2}^{x_3} \left[\sigma_{(\alpha\alpha),\alpha} + \left(1-\delta_{\alpha\beta}\right)\sigma_{(\alpha\beta),\beta}\right] \mathrm{d}\varsigma \tag{1}$$

and transverse normal stress as function of the transverse shear stress derivatives

$$\sigma_{33} = -\int_{\varsigma=-h/2}^{x_3} \sigma_{\alpha 3,\alpha}\, \mathrm{d}\varsigma. \tag{2}$$

It is assumed that the thermal load is distributed linearly through the thickness.

$$\Delta T(x_1, x_2, x_3) = T_0(x_1, x_2) + x_3 T_1(x_1 x_2). \tag{3}$$

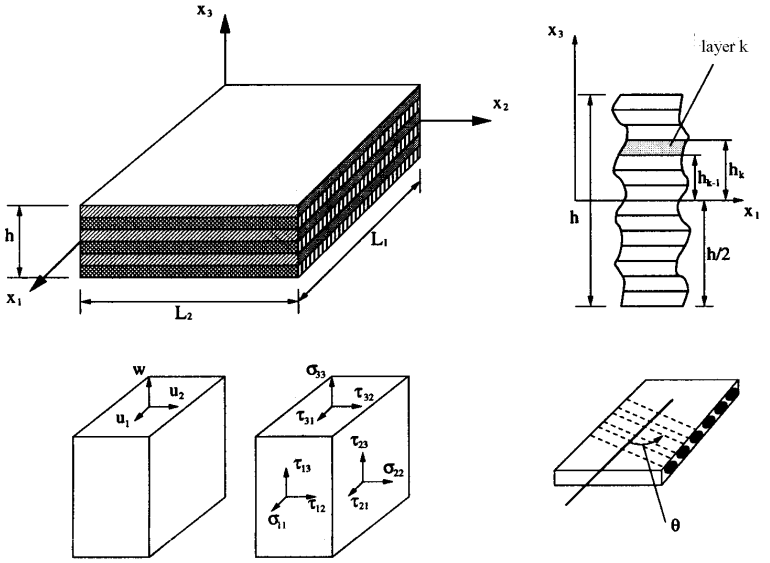

Fig. 1. Coordinate system and laminate specifications.

Introducing this assumption and the material law for a layered composite plate based on FSDT into the in-plane equilibrium conditions leads to

$$\sigma_{\alpha 3} = [\, G_{\alpha\beta\gamma\rho} \quad F_{\alpha\beta\gamma\rho}\,] \left\{ \begin{Bmatrix} N_{\gamma\rho,\beta} \\ M_{\gamma\rho,\beta} \end{Bmatrix} + \begin{Bmatrix} N^{\mathrm{th}}_{\gamma\rho,\beta} \\ M^{\mathrm{th}}_{\gamma\rho,\beta} \end{Bmatrix} \right\} - [\, a^{\mathrm{th}}_{\alpha\beta} \quad b^{\mathrm{th}}_{\alpha\beta}\,] \begin{Bmatrix} T_{0,\beta} \\ T_{1,\beta} \end{Bmatrix}, \tag{4}$$

where

$$[\, G_{\alpha\beta\gamma\rho} \quad F_{\alpha\beta\gamma\rho}\,] = -\int_{\varsigma=-h/2}^{x_3} \tilde{C}_{\alpha\beta\varepsilon\varphi} [\, 1 \quad \varsigma\,] \mathrm{d}\varsigma \begin{bmatrix} \tilde{A}_{\varepsilon\varphi\gamma\rho} & \tilde{B}_{\varepsilon\varphi\gamma\rho} \\ \tilde{B}_{\varepsilon\varphi\gamma\rho} & \tilde{D}_{\varepsilon\varphi\gamma\rho} \end{bmatrix} \tag{5}$$

and

$$[\, a^{\mathrm{th}}_{\alpha\beta} \quad b^{\mathrm{th}}_{\alpha\beta}\,] = \int_{\varsigma=-h/2}^{x_3} \tilde{C}_{\alpha\beta\gamma\rho} \alpha_{\gamma\rho} [\, 1 \quad \varsigma\,] \mathrm{d}\varsigma \tag{6}$$

with $\tilde{C}_{\alpha\beta\gamma\rho}$ being the residual stiffness coefficients of the respective layer, $\tilde{A}_{\alpha\beta\gamma\rho}$, $\tilde{B}_{\alpha\beta\gamma\rho}$, $\tilde{D}_{\alpha\beta\gamma\rho}$ the compliance coefficients of the plate, $N_{\alpha\beta}$ and $M_{\alpha\beta}$ the membrane and bending stress resultants, $N^{\mathrm{th}}_{\alpha\beta}$ and $M^{\mathrm{th}}_{\alpha\beta}$ the corresponding thermal stress resultants and $\alpha_{\alpha\beta}$ the thermal expansion coefficients. Utilizing these transverse shear stresses in the out-of-plane equilibrium condition results in the transverse normal stress

$$\sigma_{33} = \left[\, \widehat{G}_{\alpha\beta\gamma\rho} \quad \widehat{F}_{\alpha\beta\gamma\rho}\,\right] \left\{ \begin{Bmatrix} N_{\gamma\rho,\alpha\beta} \\ M_{\gamma\rho,\alpha\beta} \end{Bmatrix} + \begin{Bmatrix} N^{\mathrm{th}}_{\gamma\rho,\alpha\beta} \\ M^{\mathrm{th}}_{\gamma\rho,\alpha\beta} \end{Bmatrix} \right\} - \left[\, \widehat{a}^{\mathrm{th}}_{\alpha\beta} \quad \widehat{b}^{\mathrm{th}}_{\alpha\beta}\,\right] \begin{Bmatrix} T_{0,\alpha\beta} \\ T_{1,\alpha\beta} \end{Bmatrix}, \tag{7}$$

where

$$\begin{Bmatrix} \widehat{G}_{\alpha\beta\gamma\rho} \\ \widehat{F}_{\alpha\beta\gamma\rho} \\ \widehat{a}^{\mathrm{th}}_{\alpha\beta} \\ \widehat{b}^{\mathrm{th}}_{\alpha\beta} \end{Bmatrix} = \int_{\varsigma=-h/2}^{x_3} \begin{Bmatrix} G_{\alpha\beta\gamma\rho} \\ F_{\alpha\beta\gamma\rho} \\ a^{\mathrm{th}}_{\alpha\beta} \\ b^{\mathrm{th}}_{\alpha\beta} \end{Bmatrix} \mathrm{d}\varsigma. \tag{8}$$

These formulae make obvious that the calculation of transverse shear stresses require first derivatives of the membrane and bending stress resultants, whereas for the transverse normal stresses even second derivatives are needed. In case of a displacement approach, the shape functions therefore must allow for second and third derivatives, respectively. This constraint can be released through certain assumptions which are expected to have low influence on the transverse stresses. Such an expectation must be proved afterwards.

The extended 2D method as proposed by Rolfes and Rohwer (1997) neglects the influence of the membrane stress resultants $N_{\alpha\beta}$ and the bending moment derivatives $M_{11,2}$; $M_{22,1}$; $M_{12,1}$; $M_{12,2}$ on the transverse shear stresses. Consequently the remaining bending moment derivatives can be expressed in terms of the transverse shear stress resultants.

$$M_{(\alpha\alpha),\alpha} = Q_{\alpha}. \tag{9}$$

The transverse shear stresses then read

$$\sigma_{\alpha 3} = f_{\alpha\beta} Q_{\beta} + \left([\, G_{\alpha\beta\gamma\rho} \quad F_{\alpha\beta\gamma\rho}\,] \begin{bmatrix} A^{\mathrm{th}}_{\gamma\rho} & B^{\mathrm{th}}_{\gamma\rho} \\ B^{\mathrm{th}}_{\gamma\rho} & D^{\mathrm{th}}_{\gamma\rho} \end{bmatrix} + [\, a^{\mathrm{th}}_{\alpha\beta} \quad b^{\mathrm{th}}_{\alpha\beta}\,] \right) \begin{Bmatrix} T_{0,\beta} \\ T_{1,\beta} \end{Bmatrix}, \tag{10}$$

where $f_{\alpha\beta}$ comprises those components of $F_{\alpha\beta\gamma\rho}$ which multiply with the remaining derivatives of $M_{\gamma\rho}$ and, corresponding to the mechanical plate stiffnesses, thermal stiffnesses are defined as

$$\begin{Bmatrix} A^{\mathrm{th}}_{\alpha\beta} \\ B^{\mathrm{th}}_{\alpha\beta} \\ D^{\mathrm{th}}_{\alpha\beta} \end{Bmatrix} = \int_{\varsigma=-h/2}^{h/2} \tilde{C}_{\alpha\beta\gamma\rho}\alpha_{\gamma\rho} \begin{Bmatrix} 1 \\ \varsigma \\ \varsigma^2 \end{Bmatrix} \mathrm{d}\varsigma. \tag{11}$$

Inserting these transverse shear stresses in the out-of-plane equilibrium condition leads to the transverse normal stresses

$$\sigma_{33} = -\widehat{f}_{\alpha\beta}Q_{\alpha,\beta} - \left(\begin{bmatrix} \widehat{G}_{\alpha\beta\gamma\rho} & \widehat{F}_{\alpha\beta\gamma\rho} \end{bmatrix} \begin{bmatrix} A^{\mathrm{th}}_{\gamma\rho} & B^{\mathrm{th}}_{\gamma\rho} \\ B^{\mathrm{th}}_{\gamma\rho} & D^{\mathrm{th}}_{\gamma\rho} \end{bmatrix} + \begin{bmatrix} \widehat{a}^{\mathrm{th}}_{\alpha\beta} & \widehat{b}^{\mathrm{th}}_{\alpha\beta} \end{bmatrix} \right) \begin{Bmatrix} T_{0,\alpha\beta} \\ T_{1,\alpha\beta} \end{Bmatrix} \tag{12}$$

with

$$\widehat{f}_{\alpha\beta} = \int_{\varsigma=-h/2}^{x_3} f_{\alpha\beta}\,\mathrm{d}\varsigma. \tag{13}$$

Thus, the extended 2D method requires the transverse shear forces and their first derivatives to calculate the transverse shear and normal stresses, respectively. Therefore, in case of a displacement approach the shape functions must allow for first and second derivatives only, one derivation order less than the full equilibrium method.

2.2. Numerical experience and physical explanation

An evaluation of the extended 2D method based on the first-order shear deformation theory and improved transverse shear stiffnesses as shown by Rohwer and Rolfes (1998) and Sparr et al. (1999) has revealed that the transverse stress components are quite accurate in case of mechanical loads. That holds for cross-ply as well as for angle-ply stacking. Differences in the displacements resulting from different locations of load input (top, bottom, reference plane) lead to small deviations in the membrane stresses, which, due to the integration process, results in even smaller differences in the transverse stress components. Further test with mechanically loaded symmetric cross-ply laminated plates showed that the extended 2D method, neglecting membrane stress resultants and bending moment derivatives, delivers nearly identical results as an application of the full equilibrium equations. That also holds for thermally loaded plates as was shown in the paper by Rolfes et al. (1998b).

As compared to the 3D analysis the extended 2D method applied to plates under thermal loads in many cases delivers stresses which are good to excellent. That holds especially for the transverse shear stresses; for the transverse normal stresses, however, large differences are determined in some cases. This chapter aims at describing the numerical results and finding physical explanations for the discrepancies.

Test cases are rectangular plates where the boundary conditions

$$\begin{aligned} &u_2 = 0, \quad w = 0, \quad \varphi_2 = 0, \quad \sigma_{11} = 0 \quad \text{at } x_1 = 0, L_1, \\ &u_1 = 0, \quad w = 0, \quad \varphi_1 = 0, \quad \sigma_{22} = 0 \quad \text{at } x_2 = 0, L_2 \end{aligned} \tag{14}$$

are enforced along the edges. The quantities φ_1 and φ_2 specify the normal rotation around the axes x_2 and x_1, respectively. The plates are loaded through a temperature distribution of the form

$$\Delta T(x_1, x_2, x_3) = \overline{T}_0 \sin(\pi x_1/L_1) \sin(\pi x_2/L_2) + x_3 \overline{T}_1 \sin(\pi x_1/L_1) \sin(\pi x_2/L_2).$$

Typical high-modulus fiber composites are assumed for each individual layer the material properties of which are specified through

$$E_L/E_T = 15, \quad G_{LT}/E_T = 0.5, \quad G_{TT}/E_T = 0.3378, \quad \nu_{LT} = 0.3, \quad \nu_{TT} = 0.48,$$
$$E_T = 10.0\ \text{GPa}, \quad \alpha_L = 0.139 \times 10^{-6}\,\text{K}^{-1}, \quad \alpha_T = 9 \times 10^{-6}\,\text{K}^{-1}. \tag{15}$$

As documented in the paper by Rolfes et al. (1998b) for all cases considered, the transverse shear stresses at the edge half way between two corners obtained by means of the extended 2D method compare very well with the corresponding 3D results. Transverse normal stresses at the plate center, however, are in many cases not well determined by the extended 2D method. That holds especially for a temperature load which is constant across the plate thickness ($\overline{T}_0 \neq 0$, $\overline{T}_1 = 0$). No good agreement with the 3D results could be reached for such a loading. Only for a plate with the anti-symmetric stacking of [0,90,0,90] and a rectangular ground view ($L_2/L_1 = 2$), the transverse normal stresses show a similar distribution over the cross-section as the 3D results. In case of a linear temperature distribution $\overline{T}_1$, however, the extended 2D values compare quite well in general. Only for a symmetric stacking of $[0,90,0,90,0]_S$ and a quadratic ground view the transverse normal stresses are not satisfactory.

As a first step towards physical reasons for these somewhat strange results it must be understood why transverse normal stresses appear at all in these loading cases. Let us consider a plate consisting of one single layer subjected to a temperature load constant through the thickness ($\overline{T}_0 \neq 0$, $\overline{T}_1 = 0$). Because of the sinusoidal temperature distribution along x_1 and x_2, lentil-like deformations will appear. The same would happen for every separated slice. Fig. 2 makes obvious that compatibility of the slices require transverse normal stresses, tensile stresses near the edges and compressive ones around the plate center. Likewise, this logic holds for laminated plates with symmetric or arbitrary stacking. Orthotropy in the layer stiffnesses may only lead to differences in the stress distribution.

In case of a temperature load linearly distributed through the thickness ($\overline{T}_0 = 0$, $\overline{T}_1 \neq 0$) each separated slice would deform either into a concave or convex shape depending on its location in thickness direction. Transverse normal stresses due to compatibility between the slices appear as before but with a sign change along x_3. Consequently, the sinusoidal temperature load distribution in x_1 and x_2 will always render transverse normal stresses.

Equilibrium conditions relate transverse derivatives of the transverse normal stresses to in-plane derivatives of the transverse shear stresses.

$$\sigma_{33,3} = -\sigma_{\alpha 3,\alpha}. \tag{16}$$

At the upper and lower plate surface ($x_3 = \pm h/2$), the stresses σ_{33} must vanish. Since they cannot be zero all along x_3 as explained above, non-zero in-plane derivatives of $\sigma_{\alpha 3}$ and therewith these stresses themselves must exist. But they also must vanish at the upper and lower plate surface because of equilibrium conditions.

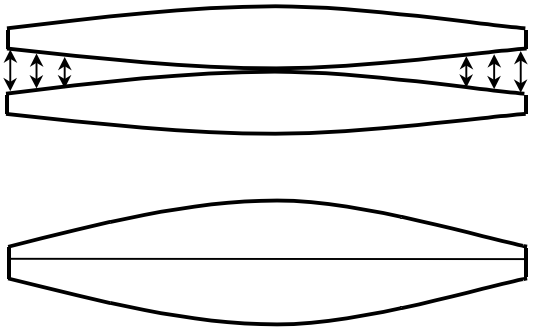

Fig. 2. Lentil-like deformations and resulting transverse normal stresses.

For a symmetrically stacked plate under a temperature load constant through the thickness ($\overline{T}_0 \neq 0$, $\overline{T}_1 = 0$), the stresses $\sigma_{\alpha 3}$ must not result in transverse shear forces when integrated over the plate thickness. Consequently the distribution along x_3 must at least have two maximum values. Using now the in-plane equilibrium conditions

$$\sigma_{\alpha 3,3} = \sigma_{(\alpha\alpha),\alpha} + (1 - \delta_{\alpha\beta})\sigma_{(\alpha\beta),\beta} \tag{17}$$

it becomes clear that a linear distribution of in-plane displacements and the resulting piece-wise linear in-plane stresses cannot adequately model the structural behavior. A higher order polynomial is necessary.

For a non-symmetric stacking as well as under a linearly distributed temperature load resulting transverse shear forces can exist. Therefore, the arguments from above do not hold anymore. But it can be assumed that also in these cases higher order polynomials would lead to a considerable improvement in the transverse shear and normal stress distribution.

3. Higher order lamination theories

3.1. Kinematics

From numerical experience and the preceding arguments it is clear that for the problem considered higher order polynomial approximations of the displacements would lead to improved transverse stresses. In order to determine necessary and sufficient polynomial degrees the displacements are developed into power series in thickness direction.

$$u_\alpha = \sum_{i=0}^{\infty} c_i u_{\alpha_i} (x_3)^i, \tag{18}$$

$$w = \sum_{i=0}^{\infty} d_i w_i (x_3)^i. \tag{19}$$

These series must be truncated so that the number of functional degrees of freedom is kept limited. Such approaches have been proposed by several authors; Table 1 lists six of them. In some cases, additional constraints are applied to reduce further the number of functional degrees of freedom. The applicability of the different theories to thermal loads, however, is seldom checked. The considered sinusoidal temperature distribution, in particular, is treated by Khdeir and Reddy (1991). But their results are restricted to transverse displacements and membrane stresses; transverse stresses are not studied.

Table 1
Higher-order theories

Theory	Polynomial degrees for i			
	$c_i = 1$	$c_i = 0$	$d_i = 1$	$d_i = 0$
Whitney and Pagano (1970) (FSDT)	0,1	>1	0	>0
Kwon and Akin (1987)	0,1	>1	0,1,2	>2
Chang and Leu (1991)	0,1	>1	0,1,3	2,>3
Khdeir and Reddy (1991)	0,1,2,3	>3	0	>0
Lo et al. (1977)	0,1,2,3	>3	0,1,2	>2
Pandya and Kant (1988)	0,1,2,3	>3	0,1,2,3	>3

In the following, results obtained by means of the FSDT will be compared against results with approaches characterized by $c_i = 1$ and $d_i = 1$ for $i = 0$–3 (HO-3) and for $i = 0$–5 (HO-5) whereas higher order terms vanish.

Standard linear strain displacement relations are assumed where the strain components are related to the displacement derivatives in the following way:

$$\varepsilon_n = \begin{bmatrix} \varepsilon_1 \\ \varepsilon_2 \\ \varepsilon_3 \\ \varepsilon_4 \\ \varepsilon_5 \\ \varepsilon_6 \end{bmatrix} = \begin{bmatrix} \gamma_{11} \\ \gamma_{22} \\ \gamma_{33} \\ \gamma_{23} \\ \gamma_{13} \\ \gamma_{12} \end{bmatrix} = \begin{bmatrix} u_{1,1} \\ u_{2,2} \\ w_{,3} \\ u_{2,3} + w_{,2} \\ u_{1,3} + w_{,1} \\ u_{1,2} + u_{2,1} \end{bmatrix}. \tag{20}$$

With the polynomial approximation of the displacements inserted the strains can also be written in the form of a polynomial series.

$$\varepsilon_n = \sum_{i=0}^{\infty} \varepsilon_{n_i} (x_3)^i. \tag{21}$$

This series is to be truncated according to the truncation of the displacement development.

In general, the kinematics described above do not meet the condition of vanishing transverse shear strains at the upper and lower plate surface. These conditions can be utilized to eliminate four functional degrees of freedom (Reddy, 1984; Kwon and Akin, 1987). If that is done, the corresponding stiffness coefficients must be modified, accordingly, which may impair the quality of the displacement distribution. Furthermore, in case of application in finite elements at least $C^{(1)}$ continuity conditions are required for the shape functions. Since, in the following, the transverse shear stresses will be determined by means of the equilibrium conditions zero transverse shear strains at the plate surfaces will not be enforced explicitly in the displacement functions.

3.2. Elasticity relation and boundary conditions

Basis for the higher-order theories is the 3D elasticity law of the layer k.

$$\begin{bmatrix} \sigma_{11} \\ \sigma_{22} \\ \sigma_{33} \\ \sigma_{23} \\ \sigma_{13} \\ \sigma_{12} \end{bmatrix}_k = \begin{bmatrix} Q_{11} & Q_{12} & Q_{13} & 0 & 0 & Q_{16} \\ & Q_{22} & Q_{23} & 0 & 0 & Q_{26} \\ & & Q_{33} & 0 & 0 & Q_{36} \\ & & & Q_{44} & Q_{45} & 0 \\ & & & & Q_{55} & 0 \\ & & & & & Q_{66} \end{bmatrix}_k \left\{ \begin{bmatrix} \gamma_{11} \\ \gamma_{22} \\ \gamma_{33} \\ \gamma_{23} \\ \gamma_{13} \\ \gamma_{12} \end{bmatrix} - \begin{bmatrix} \alpha_1 \\ \alpha_2 \\ \alpha_3 \\ 0 \\ 0 \\ \alpha_6 \end{bmatrix}_k \Delta T \right\}, \tag{22}$$

which in index notation reads

$${}_k\sigma_m = {}_kQ_{mn}\{\varepsilon_n - {}_k\alpha_n \Delta T\}. \tag{23}$$

The stresses can be integrated over the plate thickness leading to stress resultants of the form

$$N_{m_i} = \int_{(h)} \sigma_m (x_3)^i \mathrm{d}x_3. \tag{24}$$

For $i = 0,1$, these stress resultants are the standard membrane forces and bending/torsion moments; indices between 2 and 5 point to higher order stress resultants. Correspondingly, coefficients of the strain components and the components of the temperature load are to be integrated. To that end the assumed thickness distribution of the strains ε_n and the temperature load ΔT must be inserted. With

$$C_{m_i n_j} = \int_{(h)} Q_{mn} (x_3)^{i+j} \mathrm{d}x_3, \quad \text{where } i,j = 0,1,2,3,4,5 \quad \text{for HO-5} \tag{25}$$

and

$$A_{m_i \rho} = \int_{(h)} Q_{mn} \alpha_n (x_3)^{i+\rho} \mathrm{d}x_3 \quad \text{where } i = 0,1,2,3,4,5 \quad \text{for HO-5 and } \rho = 0,1, \tag{26}$$

the elasticity relation for the laminated plate reads

$$N_{m_i} = C_{m_i n_j} \varepsilon_{n_j} - A_{m_i \rho} T_\rho. \tag{27}$$

Therewith, equilibrium conditions can be established.

$$\begin{aligned} &N_{11_{i,1}} + N_{12_{i,2}} - iN_{13_{i-1}} = 0, \\ &N_{12_{i,1}} + N_{22_{i,2}} - iN_{23_{i-1}} = 0, \\ &N_{13_{i,1}} + N_{23_{i,2}} - iN_{33_{i-1}} = 0, \end{aligned} \quad \text{where } i = 0,1,2,3,4,5 \quad \text{for HO-5.} \tag{28}$$

In case of HO-5 these are 18 conditions, whereas for HO-3 the number is reduced to 12. Correspondingly, there are 2×18 and 2×12 boundary conditions to be satisfied. For a 'simple support' they can be specified as follows:

$$N_{11_i} = u_{2_i} = w_i = 0 \quad \text{at } x_1 = 0, L_1, \tag{29}$$

$$N_{22_i} = u_{1_i} = w_i = 0 \quad \text{at } x_2 = 0, L_2. \tag{30}$$

These conditions are met if the displacement functions are of the form

$$\begin{Bmatrix} u_{1_i} \\ u_{2_i} \\ w_i \end{Bmatrix} = \sum_{m=1}^{\infty} \sum_{n=1}^{\infty} \begin{Bmatrix} (\overline{u}_{1_i})_{mn} \cos(m\pi x_1/L_1) \sin(n\pi x_2/L_2) \\ (\overline{u}_{2_i})_{mn} \sin(m\pi x_1/L_1) \cos(n\pi x_2/L_2) \\ (\overline{w}_i)_{mn} \sin(m\pi x_1/L_1) \cos(n\pi x_2/L_2) \end{Bmatrix}. \tag{31}$$

3.3. Transverse stresses

The applied temperature load consists of the first term of the Fourier series only. Thus it is sufficient to restrict the displacement functions to

$$\begin{Bmatrix} u_{1_i} \\ u_{2_i} \\ w_i \end{Bmatrix} = \begin{Bmatrix} \overline{u}_{1_i} \cos(\pi x_1/L_1) \sin(\pi x_2/L_2) \\ \overline{u}_{2_i} \sin(\pi x_1/L_1) \cos(\pi x_2/L_2) \\ \overline{w}_i \sin(\pi x_1/L_1) \cos(\pi x_2/L_2) \end{Bmatrix}. \tag{32}$$

Inserting them into the strain displacement relation and using the resulting strains together with the stiffness coefficients and the temperature load in the equilibrium conditions yields a set of linear algebraic equations to determine the unknown coefficients $\overline{u}_{\alpha_i}$ and $\overline{w}_i$. They specify the complete displacement mode.

For the determination of the transverse stresses, only the membrane displacements u_{α_i} are used. In-plane derivatives are formed to derive at the membrane strains. With the aid of the material law the membrane stresses are calculated for each layer. By means of the local equilibrium conditions the in-plane derivatives of the membrane stresses are integrated to get the transverse shear stresses, whereas integrating the in-plane derivatives of these transverse shear stresses results in the transverse normal stresses.

4. Numerical application

4.1. Specification of test examples

By means of three test cases the effects discussed above are evaluated. Results obtained with the extended 2D method (FSDT), with a cubic (HO-3) and with a fifth order (HO-5) displacement approximation are compared against analytical 3D solutions. Three different lay-ups are analyzed, one single [0] layer, a four layer anti-symmetric stacking of [0,90,0,90], and a ten-layer symmetric stacking $[0,90,0,90,0]_S$. All three plates are of quadratic shape with a slenderness ratio of $s = L/h = 5$. This rather small ratio is chosen to make the differences between the theories more visible. Even smaller values are not suitable because of increased influence of boundary layer that effects along the 'simply supported' edges.

Material properties and loading conditions are identical to those specified in Section 2.2. Transverse shear stresses σ_{13} and σ_{23} are determined at the mid-side edge points $(0; L_2/2)$ and $(L_1/2; 0)$, respectively, whereas the transverse normal stresses σ_{33} are calculated at the plate center $(L_1/2; L_2/2)$. Due to the applied thermal load and the boundary conditions these are the points where the stresses reach maximum values. The stress distribution in x_1- and x_2-direction follows harmonic functions.

4.2. Single layer [0] plate

One single layer is actually not a layered structure. Such a plate is included to study the effect of the sinusoidal temperature distribution separately.

For a thermal load constant through the thickness ($\overline{T}_0 \neq 0$, $\overline{T}_1 = 0$) Fig. 3 shows the expected roughly cubic distribution of transverse shear stresses. Larger values of σ_{13} as compared to σ_{23} are due to the higher modulus values of G_{LT} and E_L as compared to G_{TT} and E_T, respectively. Transverse normal stresses σ_{33} show compression at the plate center which confirms the reflections based on the lentil-like deformations.

The extended 2D method (FSDT) delivers zero stresses across the plate thickness. That can be traced back to the fact that no transverse shear forces are involved, and the derivatives of the thermal load distribution vanish at the mid-side edge points as well as at the plate center. The cubic displacement approximation yields results which model the stress distribution quite well; only the maximum values are somewhat too large. With the fifth order polynomials, however, there is hardly any difference to the 3D solution any more.

Thermal loads distributed linearly over the plate thickness ($\overline{T}_0 = 0$, $\overline{T}_1 \neq 0$) result in a bending deflection. The applied boundary conditions then lead to transverse shear forces. The shear forces at the edges parallel to x_1 must be of opposite sign to those at the edges parallel to x_2. That is reflected by the positive stresses σ_{13} and the negative values of σ_{23}. Transverse normal stresses are rather small, with compressive values in the upper half and tensile ones in the lower half. They can be explained by the compatibility constraints of concave and convex deformation shapes of separated slices.

Transverse shear stresses obtained through the extended 2D method are rather accurate. That especially holds for σ_{23}, where the shape as well as the maximum value correspond very well with the exact results. For σ_{13}, the maximum value is about 9.5% too large and the shape is somewhat too pointed. The generally good correspondence can be traced back to the influence of transverse shear forces at the edges which are used to calculate the stresses in the extended 2D method. For transverse normal stresses σ_{33}, zero values are determined. That is due to the fact that the transverse shear force derivatives vanish at the plate center. The cubic displacement approximation yields results which deviate only slightly in case of the maximum values for σ_{33}, whereas the fifth order polynomials determine hardly any difference to the 3D solution.

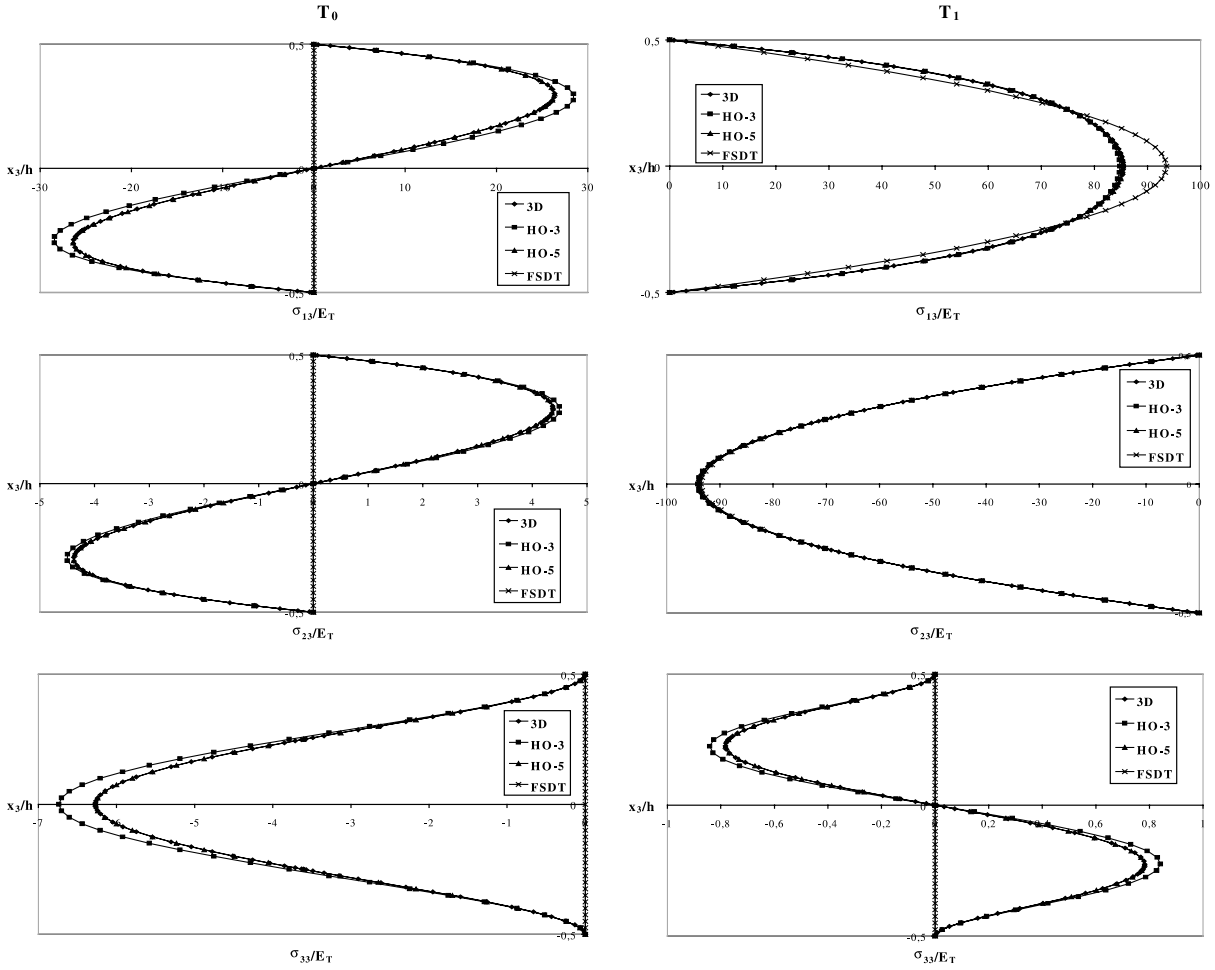

Fig. 3. Transverse stresses in a single layer [0] plate.

4.3. Anti-symmetric [0,90,0,90] plate

Fig. 4 depicts the transverse stresses determined for the anti-symmetric laminate of [0,90,0,90]. Such a lay-up leads to a bending deformation even for the constant thermal load ($\overline{T}_0 \neq 0$, $\overline{T}_1 = 0$). Transverse shear forces must develop at the edges. That is reflected by the transverse shear stresses σ_{13} and σ_{23}. Their zig-zagging mode can be explained by abrupt stiffness changes between the 0°- and the 90°-layers. Values of σ_{13} and σ_{23} are of opposite sign but exactly central symmetric in magnitude. Transverse normal stresses σ_{33} are compressive at the plate center. That again is due to compatibility constraints in connection with the lentil-like deformations.

With the extended 2D method (FSDT) the zig-zagging modes of the transverse shear stresses are well captured. Though the values are somewhat off, they still show exact central symmetry. The transverse normal stresses, however, are determined as tensile, their distribution differs drastically from the 3D results. Cubic and fifth order displacement approximations deliver transverse stresses which are nearly identical to the 3D solution.

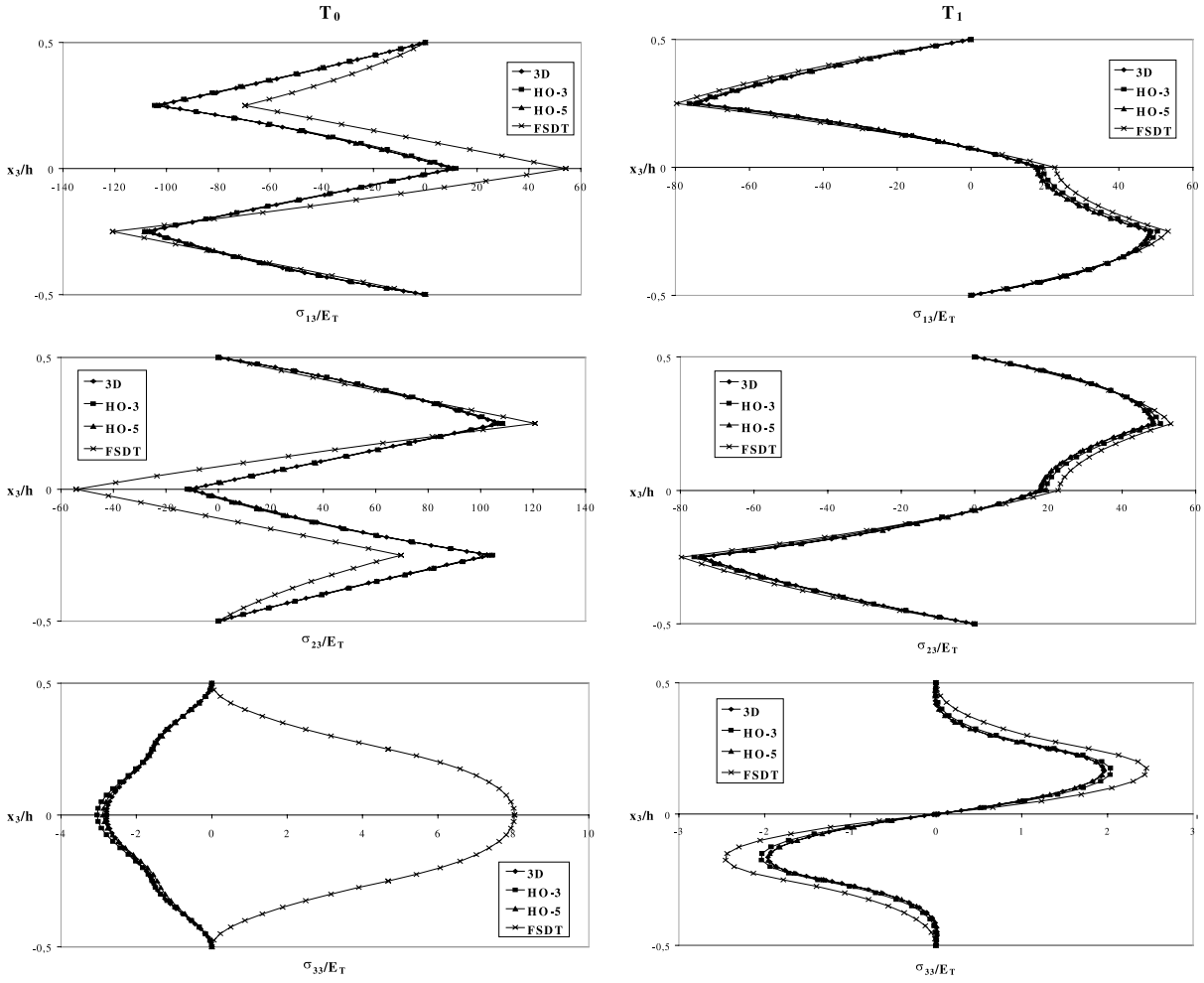

Fig. 4. Transverse stresses in an anti-symmetric [0,90,0,90] plate.

Through linearly distributed thermal loads ($\overline{T}_0 = 0$, $\overline{T}_1 \neq 0$) additional bending is induced. Fig. 4 shows that it results in transverse shear stresses which are of opposite sign in the upper and lower half of the plate. The distribution of σ_{13} in positive x_3-direction is exactly the same as that of σ_{23} in negative x_3-direction. For σ_{33} the dependency in thickness direction is similar to that of the single layer plate under linear temperature load, though with opposite sign. The relatively small contribution due to the compatibility constraints of concave and convex deformation shapes of separated slices must be superimposed by larger transverse normal stresses due to bending.

Distribution shapes of transverse shear and normal stresses are rather well captured by the extended 2D method (FSDT). Maximum values of the normal stresses, however, exceed those of the 3D results by about 25%. Results of the cubic displacement approximation are much more accurate, and the fifth order approach show hardly any difference to the exact solution.

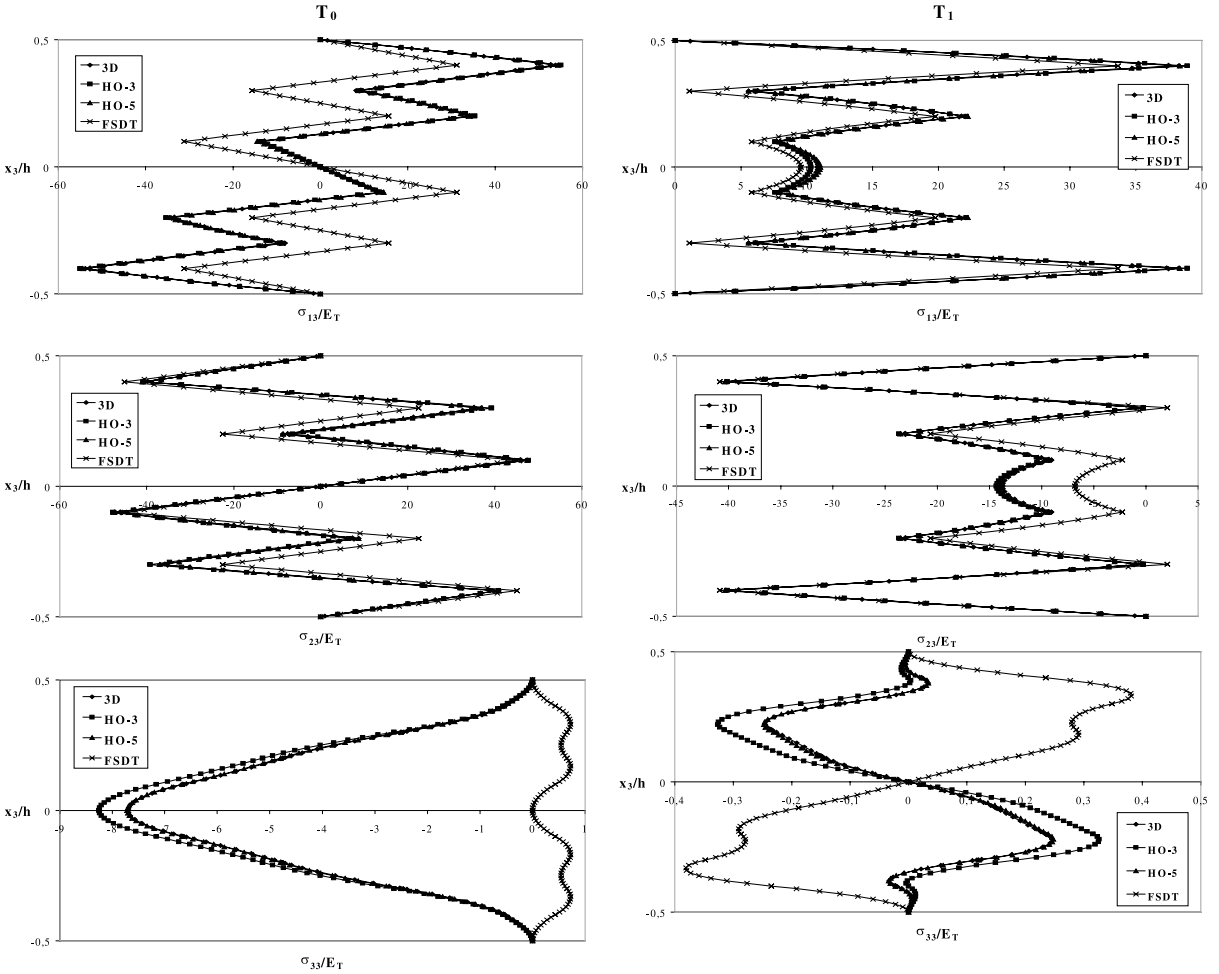

Fig. 5. Transverse stresses in a symmetric $[0,90,0,90,0]_S$ plate.

4.4. Symmetric $[0,90,0,90,0]_s$ plate

Results obtained for the ten-layer symmetric laminated are given in Fig. 5. Constant temperature through the thickness ($\overline{T}_0 \neq 0, \overline{T}_1 = 0$) leaves the symmetry plane straight. But the sinusoidal distribution in x_1 and x_2 causes the lentil-like deformation as described before. Each layer undergoes bending deformation, and because of the abrupt stiffness changes between the 0°- and the 90°-layers transverse shear stresses appear in a zig-zagging mode. Distribution through the thickness of σ_{13} as well as of σ_{23} is exactly central symmetric. At the plate center compressive normal stresses σ_{33} show roughly the same distribution as for the single layer plate.

Again, the extended 2D method (FSDT) captures the central symmetric zig-zagging shape of the transverse shear stresses quite well, though the values, especially for σ_{23}, are somewhat off. But as in the single layer plate the transverse normal stresses are in no way comparable with the exact results. Cubic and fifth order approximation result in transverse shear stresses which hardly deviate from the 3D solution.

Only for σ_{33}, the maximum value at the plate center is 7.1% too large, whereas the fifth order approximation result is again very close to the 3D value.

Under a linear temperature distribution ($\overline{T}_0 = 0$, $\overline{T}_1 \neq 0$), the bending deformation results in positive values for σ_{13} and corresponding negative values for σ_{23}. With exception of the two central 0°-layers they are again zig-zagging forms, but now symmetric with respect to the center plain. In general, the transverse normal stress distribution are comparable to those obtained for the single layer plate. Only in the outer 0°-layers the stresses tend towards a different form. That can be traced back to bending overlaying the lentil-like deformations.

The shear stress σ_{13} especially is quite well modeled by the extended 2D method (FSDT), σ_{23} is much worse. That is because of the larger membrane and bending stiffness in x_1-direction as compared to x_2. The transverse normal stresses by the extended 2D method capture only the bending effect, not the lentil-like deformations and is therefore no way near the exact results. The cubic approximation (HO-3) delivers rather accurate transverse shear stresses, whereas the normal stresses are 33% too large at the maximum. All results from the fifth order approximation compare very well with the exact results.

5. Conclusion

Former investigations have shown that the extended 2D method as proposed by Rolfes and Rohwer (1997), Rolfes et al. (1998a), yields excellent results in the case of mechanical loads applied to plates with cross-ply as well as with angle-ply stacking. Also under thermal loads very good results could be obtained. Only in some cases, the proposed method led to transverse shear and especially transverse normal stresses which were far off the exact solution.

In this study the discrepancies could be traced back to temperature load of the form

$$\Delta T(x_1, x_2, x_3) = \overline{T}_0 \sin(\pi x_1/L_1) \sin(\pi x_2/L_2) + x_3 \overline{T}_1 \sin(\pi x_1/L_1) \sin(\pi x_2/L_2).$$

Such a temperature distribution leads to lentil-like deformations which cannot be captured by the 2D method. For cross-ply laminates it has been shown that higher order approximations with cubic and fifth order polynomials for the displacement distribution in thickness direction leads to much better results. Further investigations would be necessary to verify these findings also for plates with angle-ply stacking.

It should be noticed, however, that the number of functional degrees of freedom involved with these higher order approximations is considerably larger as compared to the 2D method, leading to a much higher computational effort. This higher effort should be restricted to cases where really needed. From the results presented it is evident that only in cases of temperature loads varying considerably in the direction of the reference surface the extended 2D method is not sufficient and cubic or fifth order polynomials should be used to approximate the displacement distribution in thickness direction.

References

Chang, J.S., Leu, S.Y., 1991. Thermal buckling analysis of antisymmetric angle-ply laminates based on a higher-order displacement field. Composite Sci. Tech. 41, 109–128.

Chaudhuri, R.A., 1986. An equilibrium method for prediction of transverse shear stresses in a thick laminated plate. Comput. Struct. 23, 139–146.

Gruttmann, F., Wagner, W., 1994. On the numerical analysis of local effects in composite structures. Compos. Struct. 29, 1–12.

Khdeir, A.A., Reddy, J.N., 1991. Thermal stresses and deflections of cross-ply laminated plates using refined plate theories. J. Thermal Stresses 14, 419–438.

Kwon, Y.W., Akin, J.E., 1987. Analysis of layered composite plates using high-order deformation theory. Comput. Struct. 27, 619–623.

Lo, K.H., Christensen, R.M., Wu, E.M., 1977. A high-order theory of plate deformation (Part 2: laminated plates). J. Appl. Mech. 44, 669–676.

Malik, M., Bert, C.W., 1998. Three-dimensional elasticity solution for free vibration of rectangular plates by the differential quadrature method. Int. J. Solids Struct. 35, 299–318.

Mau, S.T., Tong, P., Pian, T.H.H., 1972. Finite element solutions for laminated thick plates. J. Compos. Mater. 6, 304–311.

Noor, A.K., Burton, W.S., Peters, J.M., 1990. Predictor–corrector procedures for stress and free vibration analyses of multilayered composite plates and shells. Comput. Meth. Appl. Mech. Engng. 82, 341–363.

Noor, A.K., Burton, W.S., 1990. Three-dimensional solutions for antisymmetrically laminated anisotropic plates. J. Appl. Mech. 57, 182–188.

Noor, A.K., Malik, M., 2000. An assessment of five modeling approaches for thermo-mechanical stress analysis of laminated composite panels. Computat. Mech. 25, 43–58.

Owen, D.R.J., Li, Z.H., 1987. A refined analysis of laminated plates by finite element displacement method – I. Fundamentals and static analysis. Comput. Struct. 26, 907–914.

Pagano, N.J., 1970. Exact solutions for rectangular bidirectional composites and sandwich plates. J. Compos. Mater. 4, 20–34.

Pandya, B.N., Kant, T., 1988. Flexural analysis of laminated composites using refined higher-order C^0 plate bending elements. Comput. Meth. Appl. Mech. Engng. 66, 173–198.

Reddy, J.N., 1984. A simple higher-order theory for laminated composite plates. J. Appl. Mech. 51, 745–752.

Robbins Jr., D.H., Reddy, J.N., 1993. Modelling of thick composites using a layerwise laminate theory. Int. J. Numer. Meth. Engng. 36, 655–677.

Rohwer, K., 1988. Improved transverse shear stiffness for layered finite elements. DFVLR-Forschungsbericht 88-32, Braunschweig.

Rohwer, K., 1992. Application of higher order theories to the bending analysis of layered composite plates. Int. J. Solids Struct. 29, 105–119.

Rohwer K., Rolfes, R., 1998. Calculating 3D stresses in layered composite plates and shells. Mech. Compos. Mater. 34, 491–500.

Rolfes, R., Rohwer, K., 1997. Improved transverse shear stresses in composite finite elements based on first-order shear deformation theory. Int. J. Numer. Meth. Engng. 40, 51–60.

Rolfes, R., Rohwer, K., Ballerstaedt, M., 1998a. Efficient linear transverse normal stress analysis of layered composite plates. Comput. Struct. 68, 643–652.

Rolfes, R., Noor, A.K., Sparr, H., 1998b. Evaluation of transverse thermal stresses in composite plates based on first-order shear deformation theory. Comput. Meth. Appl. Mech. Engng. 167, 355–368.

Sparr, H., Rohwer, K., Rolfes, R., Taeschner, M., 1999. Anwendung einer Schubverformungstheorie höherer Ordnung auf thermo-elastische Plattenprobleme. DLR Internal Report IB 131-99/19, Braunschweig.

Spilker, R.L., Chou, S.C., Orringer, O., 1977. Alternate hybrid-stress elements for analysis of multilayer composite plates. J. Composite Mater. 11, 51–70.

Spilker, R.L., 1982. Hybrid-stress eight-node elements for thin and thick multilayer laminated plates. Int. J. Numer. Meth. Engng. 18, 801–828.

Srinivas, S., Rao, A.K., 1970. Bending, vibration and buckling of simply supported thick orthotropic rectangular plates and laminates. Int. J. Solids Struct. 6, 1463–1481.

Vel, S.S., Batra, R.C., 1999. Analytical solution for rectangular thick laminated plates subjected to arbitrary boundary conditions. AIAA-J. 37 (11), 1464–1473.

Whitney, J.M., Pagano, N.J., 1970. Shear deformation in heterogeneous anisotropic plates. J. Appl. Mech. 37, 1031–1036.